Journal of Archaeological Science 102 (2019) 11–25

Contents lists available at ScienceDirect

Journal of Archaeological Science

journal homepage: www.elsevier.com/locate/jas

At the water's edge: Micromorphological and quantitative mineral analysis of a submerged Mesolithic shell midden at Hjarnø Sund, Denmark

Ingrid Ward[a,b,*], Peter Moe-Astrup[c], Kelly Merigot[d]

[a] College of Humanities, Arts and Social Sciences, Flinders University, GPO Box 2100, Adelaide, SA, 5001, Australia
[b] School of Social and Cultural Studies, University of Western Australia, 35 Stirling Highway, Crawley, WA, 6009, Australia
[c] Moesgaard Museum, Moesgaard Alle 15, 8270, Højbjerg, Denmark
[d] John de Laeter Centre, Faculty of Science & Engineering, Curtin University, Bentley, WA, 6102, Australia

ARTICLE INFO

Keywords:
Shell midden
Submerged landscapes
Micromorphology
Archaeology
Automated mineral analysis
TIMA

ABSTRACT

This study presents the first application of micromorphology and Automated Scanning Electron Microscopy (ASEM) to a submerged shell-bearing midden site in Denmark, one of the few submerged shell-matrix sites in the world to have undergone archaeological excavation. The use of micromorphology in these deposits provides a means to distinguish primary and secondary deposits and degree of preservation. The additional input of quantitative mineral analysis provides an empirical tool for correlation of minerogenic components across the site and assessing change through time. Micromorphological insights into the formation history and post-depositional modification include epizootic infestations within oyster shells at the base of the profile and needle-fibre calcite at the top - the former is indicative of accumulation of at least part of the shell midden below water, whilst the latter is indicative of exposure. Aside from the shell itself, other cultural traces include heated and worked flint fragments, burnt and unburnt hard bone fragments (including fish bone), soft (spongy) bone, charcoal (*Ulmus* sp., *Alnus* sp., *Corylus* sp.), and preservation of what could possibly be antler velvet. Quantitative mineral analyses provide support for the successive stabilisation of the midden site by accumulating minerogenic (silica-rich) sands over the glacial clay and detrital gyttja deposits (defined by smaller grain size, greater heavy mineral content), and subsequently between the shell matrix itself, until the erosion of these protective sediments in more recent times. Further micromorphological profiles are needed to fully assess local versus regional signatures within the site, which otherwise provides an ideal context against which to compare the effects of inundation in similar microtidal contexts.

1. Introduction

The Late Mesolithic Ertebølle shell middens or kitchen middens (*køkkenmodding*) of Denmark have been a focus for interdisciplinary research for over a century partly because of their relative visibility and partly because of the many well-preserved cultural and faunal remains within them (Anderson, 2000, 2004; Bailey et al. in press). Over 350 of these midden sites are found above water in northern Denmark as a result of relative uplift associated with ongoing glacio-isostatic adjustments following the melting of the Fennoscandic ice-cover (Anderson, 2000, 2013, see also Rosentau et al., 2017). In southern Denmark, many hundreds of Stone Age sites are now under water, including 37 submerged Mesolithic find spots in the Horsens Fjord system alone (Fig. 1). Few if any of these submerged sites are confirmed shell middens and even fewer have been systematically excavated - only Tybrind Vig, Ronæs Skov, Argus Grund and Møllegabet II (Bailey et al. in press). In the absence of focused excavation and analysis, it remains unclear whether these shell deposits are *in situ* or have been re-deposited by marine inundation, although their preservation is generally favoured by the protective coastlines and low energy (limited wind fetch, and reduced wave height) conditions in inner Danish waters (Rosentau et al., 2017).

One other site to have undergone detailed archaeological investigation is the Stone Age shell-matrix site of Hjarnø Sund (Skriver et al., 2017; Astrup et al. submitted). The site of Hjarnø Sund is located in a water depth of 0.5–2 m on the western shore of the small island ($3.2\ km^2$) of Hjarnø in the outermost part of Horsens Fjord (Fig. 1). The site was originally situated next to a shallow coastal lagoon represented by deposits of gyttja (Skriver et al., 2017). The midden itself lies across a sloped sequence seaward of a shallow $20\ m^2$ bank (Fig. 1), comprised of glacial clay and overlain by sand, with one end of the midden unconformably overlying glacial clay and the other overlying gyttja

* Corresponding author. College of Humanities, Arts and Social Sciences, Flinders University, GPO Box 2100, Adelaide, SA, 5001, Australia.
E-mail address: ingrid.ward@uwa.edu.au (I. Ward).

https://doi.org/10.1016/j.jas.2018.12.009
Received 8 August 2018; Received in revised form 12 December 2018; Accepted 17 December 2018
Available online 04 January 2019

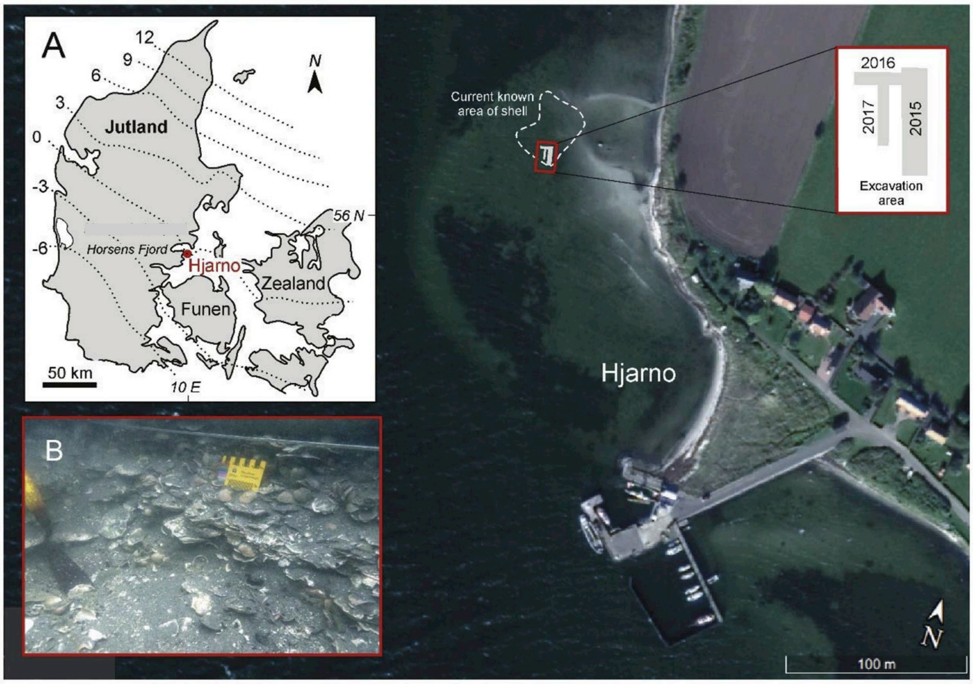

Fig. 1. Google map showing location of the Hjarnø Sund site next to a shallow bank off the island of Hjarno on the east coast of Denmark. Excavations (2015-2017) are sited on the southern part of the current known area of shell (dashed lines) as based on augering transects. Inset map (A) shows isobases in metres (dotted lines) for the highest level of the Littorina Sea (ca. 6200 yrs BP) above present sea-level (after Astrup et al. submitted). Inset (B) shows west wall of midden excavation.

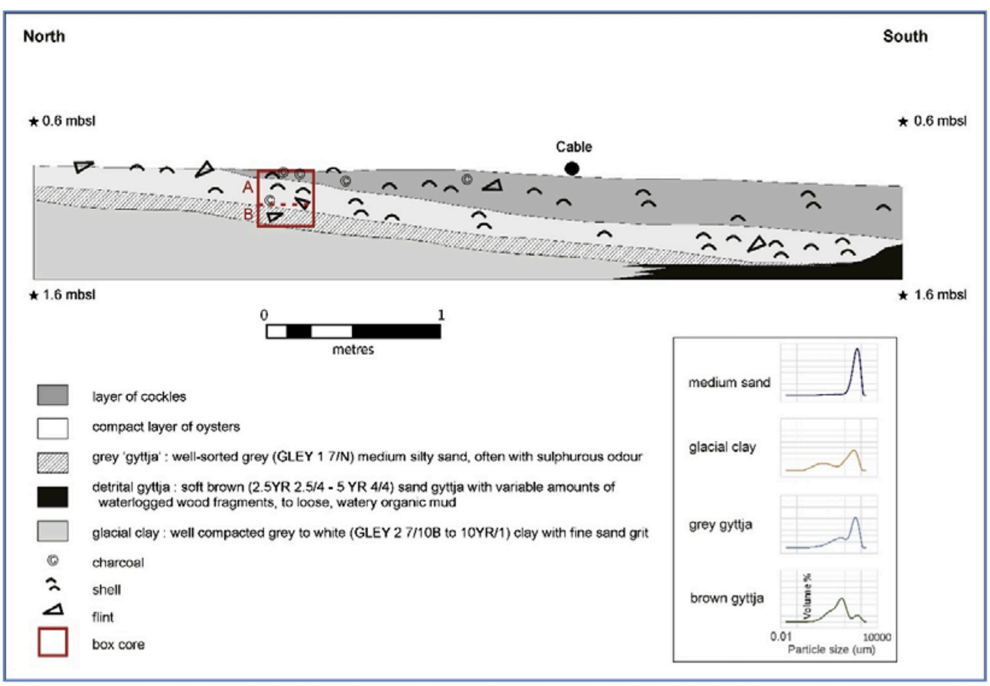

Fig. 2. Interpreted stratigraphy at midden site showing (sourced from Astrup et al. submitted). The midden site occurs across a slope, with one end overlying glacial clay and the other overlying gyttja.

(Fig. 2). Underwater excavation and sediment coring undertaken between 2013 and 2017 has revealed a rich collection of material ranging in age from the Early Ertebølle (~7300 BP) to the Middle Ertebølle (~6500 BP) (Skriver et al., 2017; Astrup et al. submitted) and is argued by Larsen et al. (2018) to be one of the oldest-known submerged midden sites in Denmark.[1]

The stratified deposit included layers of edible shell species including mainly oysters (*Ostrea edulis*), as well as cockles (*Carastoderma edule*), mussels and periwinkles (*Littorina littorea*). Current age estimates of the cockle shells range from 7245 to 6905 cal BP (Astrup et al. submitted), which overlap but are offset by ~100 yrs from the oyster chronology. This corresponds with previous dating analyses on the Hjarnø site that indicate the oyster-to-cockle shift is chronologically consecutive (separated by as little as 0–163 yr) (Larsen et al., 2018). The layers also contained large amounts of worked flints, charcoal, fish remains and mammals bones, including whale and roe deer (*Capreolus*

[1] Earlier dates of 7920–7520 BP are reported for the submerged Argus Bank site (Fischer et al., 2007) but this is not a midden site.

capreolus). Above and below the shell are layers of gyttja, from which artefacts such as painted paddles, dugout canoes, axes, bows, and fishing implements of bone, antler and wood have been recovered (Skriver et al., 2017).

In June 2017, a joint Australian-Danish team undertook further investigation of the Hjarnø shell-matrix site (Fig. 1) as part of the *Deep History of Sea Country* project (Benjamin et al., 2018; Astrup et al. submitted). The 2017 investigations of Hjarnø Sund included a combination of excavation, photographic and photogrammetric recording, geophysical survey, sediment coring and collection of samples for archaeological, geochronological, sedimentological and soil micromorphological analysis – the latter of which is the focus of this paper. As with previous excavations, virtually all layers in the midden contain flint artefacts, fish bones, hazelnuts, charcoal and an in-situ hearth feature that further attests its anthropogenic origins (Astrup et al. submitted).

Whilst evidence for the cultural origin of the shell-matrix site is strong, there remains some question as to the formation history and post-depositional disturbance of the site by marine erosion (see also Astrup et al. submitted). One means to assess this is through micromorphology, here supplemented by Automated Scanning Electron Microscopy (ASEM) to further aid the identification of minerals and sedimentary processes within these midden deposits (see also Ward and Maksimenko, 2019). Micromorphology has been successfully applied to terrestrial midden sites (e.g. Villagran et al., 2011; Mijares, 2016) and also to submerged wetland and lake dwelling deposits (Lewis, 2007; Ismail-Meyer, 2014). However, the micromorphological investigation of marine inundation on archaeological sites is limited, with the only known published study (Macphail et al., 2010) undertaken on arable and grassland sites rather than coastal sites. This study presents the first application of micromorphology and quantitative mineral analysis to a submerged shell-matrix site, and thus offers a new and comparative analysis of natural and cultural formation processes within these types of deposits.

2. Methods

2.1. Micromorphology

Sampling for archaeological micromorphology was undertaken by underwater archaeologists during the 2017 investigations of Hjarnø Sund. The 5 × 1 m long excavation runs parallel to the 2015 excavation (Fig. 1), with 1 m^2 excavation squares excavated by arbitrary units until basal clays were reached. Further details on excavation and survey methods are provided by Astrup et al. (submitted). The sampling strategy for micromorphology involved two sets of samples: (1) a 5 cm diameter x 50 cm long PVC tube core taken ~ 4 m southeast of the midden excavation site, and (2) a series of two box cores (30 × 30 × 10 cm), one immediately below the other, on the eastern side of the second 1 m^2 excavation square (Fig. 2). The former was taken with the aim of sampling the gyttja-shell transition as this was not present in the excavation itself. In addition, representative sediments were collected by coring from the different sediment facies around the midden site. Sediments were also sampled at 2–4 cm intervals down the box core profile.

The central part of the topmost box core (Box Core A) contained a hearth-like feature (Fig. 3). This central part extracted by cutting away the surrounding sediment, which was retained for associated sedimentological analyses. The remaining 'heart' was wrapped in plaster (Fig. 3) and transported to the University of Western Australia (UWA) for resin impregnation (Inset Fig. 3C) and later micromorphological analysis. Two kubiena tins were used to obtain undisturbed sub-samples of the second box core (Inset Fig. 3C and D). The < 2 mm fraction from collected sediment samples were analysed by laser particle size analysis (using Malvern Mastersizer 2000, v 5.6) at UWA.

Large (5 × 7 cm) thin-sections from the box cores' were produced by Spectrum Petrographics, Vancouver, USA, whilst standard (2.5 × 5 cm) thin sections from the tube core were produced at UWA. Thin sections were analysed at the Archaeology Department, UWA, using a Nikon petrographic microscope at magnifications ranging from 2.5x to 50x, under plane polarized (PPL) and cross polarized (XPL) light. Identification of cultural components, including shell, bone, charcoal and ashes, were made using available reference literature (e.g. Stoops et al., 2010; Nicosia and Stoops, 2017).

2.2. Automated Scanning Electron Microscopy

The eight micromorphological thin sections were analysed by Automated Scanning Electron Microscopy (ASEM) using a TESCAN Integrated Mineral Analyzer (TIMA-X) system at the John de Laeter Centre, Curtin University, to obtain quantitative mineral analyses of the different sedimentary layers. ASEM analyses were conducted at operating conditions of 25 keV using a spot size of 52 nm, a working distance of 15 mm, with a pixel spacing of 10 μm and a field size set at 1500 μm. Modal mineralogy was determined using Version 1.5 TIMA software and presented in terms of pixel area percentages), from representative sets of 5 × 5 fields (7500 μm × 7500 μm) from each of the stratigraphic layers or from the full slide. Mineral identifications are defined by chemical composition and mineral structure as determine from TIMA analyses, using a standard (Astimex Scientific MINM25 + 53 + FC mineral standard Serial 1AQ). Further details on the TIMA operating system can be found in Hrstka et al. (2018), with useful discussions on the application of ASEM to geoarchaeology can be found in Haberlah et al. (2011), Knappett et al. (2011) and Ward et al. (2018).

3. Results

3.1. Hjarnø Sund sediment facies

As outlined above, the Hjarnø shell-matrix site forms part of a sloped and deepening sequence over a glacial clay bank. The clay bank is overlain by a layer of coarse unimodal sands, with variable amounts of reworked shell (mainly *Cardium* sp. and *Mytilus* sp.) and reworked cultural material (Table 1). The wider area is covered by poorly-sorted coarse sands with variable amounts of pebbles. These gravelly sands are concentrated around the south–south-western edge of the clay bank, presumably as a result of higher current and/or wave energy. Further offshore, the transition is to grey gyttja[2] at 20–60 cm depth, brown, detrital gyttja and then fine detrital gyttja in the deeper parts of the section, south of the main midden site (Table 1). Within the detrital gyttja are fragments of waterlogged wood, mainly hazel. Grey gyttja is comprised of well-sorted medium grained silty sands that in some parts have a distinct sulphurous odour indicative of anoxic conditions. The shell midden excavated in 2017 overlies this grey gyttja, which itself unconformably overlies culturally sterile moraine clay.

Taken on the northeastern edge of the 2017 excavation, the box core sample (Box Core B) shows a transition from the grey gyttja sediments at the base to a slightly darker (GLEY 1 7/N) unit (5 cm thick) of grey silty sands, with minor shell fragments and a few pebbles. The top of Box Core B overlaps with the oyster (*Ostrea edulis*) layer (7–9 cm thick) from Box Core A, which defines the midden proper. The oyster shells tend to be oriented slightly inclined to horizontal and concave-down in a hydrodynamic stable orientation (Fig. 4). A large flint fragment, shown in Fig. 3B, is present near the top of this thick oyster unit. Above the oyster layer is a thin (1–2 shell thick) mussel (*Mylitus edulis*) layer, over which is a layer (< 5 cm thick) of cockle (*Cerastoderma edule*) shells, either inclined or horizontal concave-up, mixed with a few oyster

[2] Strictly speaking this unit is not a gyttja as it does not contain the minimal amount of organic matter (Mörner, 1982).

Fig. 3. (A) Box core A taken around a charcoal feature from upper part of the 2017 midden excavation, with inset (B) showing resin impregnated core with embedded flint artefact. (C) Box core B from lower part of midden site and (D) position of Kubiena samples from Box Core B.

Table 1
Description of main sediment facies. Distinction is made between detrital gyttja (with remaining cellular structures), which occurs in shallow water, and fine detrital gyttja (fine organic particles without remaining cellular structures) form, which forms in deeper water (Mörner, 1982).

Facies	Short Descriptor	Munsell colour	Modal peak	Description
1	Medium sand	GLEY 1 7/N to 6/N (darker = charcoal)	450 µm	Generally unimodal medium grey sand with variable amounts of reworked shell
2	Grey gyttja	GLEY 1 7/N	445 µm, 60 µm	Well-sorted grey medium silty sand, often with distinct sulphurous odour
3a	Brown (detrital) gyttja	2.5 YR 4/4 to 5 YR 4/4	60 µm, 550 µm	Soft brown sandy gyttja with variable amounts of waterlogged wood-fragments
3b	Fine detrital gyttja	2.5 YR 2.5/4	60–100 µm	Loose, watery organic brown mud
4	Glacial clay	GLEY 2 7/10B to 10YR/1	340 µm, 5 µm	Well compacted grey to white clay with fine sand grit

and mussel shells (Fig. 4). This orientation of shell, or lack thereof, may imply human discard (e.g. Claassen, 1998; Henderson et al., 2002) and/or greater bioturbation of these uppermost sediments (Salazar-Jimenez et al., 1982). Towards the top of the box core, the interstitial sands become increasingly charcoal-rich, giving a darker colour to the matrix (Table 1). The topmost charcoal feature comprises well-sorted medium-fine dark grey to black (GLEY 1 8/N) sands with large fragments (0.5–1 cm) of charcoal, and a large 2.5 cm flint fragment.

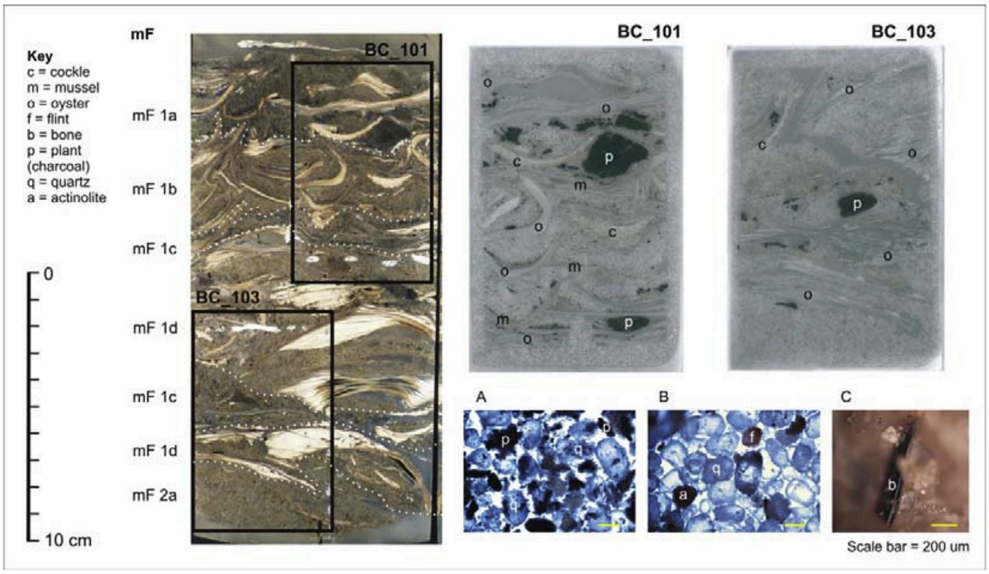

Fig. 4. Micromorphological sections BC_101 and BC_103 from Box Core 1, and scanned images of corresponding thin sections. Interpreted microfacies (mF) within the midden profile are shown as white dotted lines. Also shown are reflective microscope images of (A) charcoal inclusions in poorly sorted sediments at top of profile, (B) moderate to well-sorted sediments in the central part of the profile, and (C) burnt bone observed at the base of profile.

Table 2
Summary of modal peak as determined by Mastersizer, and median grain size (μm) for quartz and orthoclase as determined by ASEM, and also porosity (volume %) as determined by ASEM.

	Modal peak (μm)	Quartz (μm)	K-feldspar (μm)	Porosity %
Tube Core				
TC101	nd	414	256	5
TC102	nd	338	170	11
TC103	nd	440	142	10
TC104	nd	140	77	10
Box Core				
BC101	450	371	259	3
BC103	460	359	283	3
BC201	440	343	244	2
BC202	415	341	195	4

4. Microstratigraphy - Tube sample

4.1. ASEM analyses

The tube profile taken adjacent to the main midden excavation shows three of the four main stratigraphic units (SU) or facies, which are summarised in Table 3 and presented in Fig. 5. The assemblage of minerals identified in thin sections is similar throughout the sequence, comprising mainly quartz, carbonate (mainly shell), feldspar, amphibole and heavy minerals. However, the modal abundance of these minerals changes downward through the profile as indicated from the quantitative mineral results (Fig. 5). This shows a decrease in relative percentage of quartz (from ~70% to 20%) and increase in carbonate – mainly as shell (from 12% to 44%) and fine calcite (0.4%–1.1%), reflecting the decrease in interstitial sand through the main shell midden units. ASEM results also show a decrease in the median grain size of quartz (from 480 μm to 260 μm) and orthoclase (from 300 μm to 70 μm), the most abundant silicate minerals, downwards through the shell units (Table 2). Larger clasts are predominantly charcoal and flint, the latter including some artefactual remains.

The minerogenic component increases in the underlying sands, with higher relative percentages of quartz (73%), orthoclase (~6%), plagioclase (0.25%) feldspar, muscovite (0.17–23%) and amphibole (0.14–0.4%) and almost negligible carbonate (< 1%). The anoxic conditions of these sands are reflected in the higher relative percentages of pyrite (0.19–28%). In the underlying gyttja, both the relative percentage (~50%) and the median grain size (150 μm) of quartz, as well as carbonate (< 0.2%), is at its lowest. As might be expected, the content of defined plant (4%) and pyrite (0.55%) is high in this unit. Most notable is the significantly greater content (28%) of what has been defined as rock flour – a very fine-grained silica-rich phase and heavy minerals including zircon, ilmenite, titanate and rutile that most likely reflect some input from the underlying glacial clay. Porosity is greatest in the lower units (10–11%) and is lowest in the top-most unit (5%, Table 2) possibly reflecting the coarser grain size. The micromorphological description of each of the units is described below.

4.2. Stratigraphic unit 1 (Samples TC101, TC102)

This unit is equivalent to the main shell-bearing midden unit as presented in Box Core A. In the tube core it is approximately 20 cm thick, with a sharp transition between the shell layers and the underlying sands (Fig. 6). This unit has an even c/f (coarse:fine) ratio and single grain to pellicular microstructure comprising well-sorted, mainly sub-rounded medium sands with a very fine sand component (Table 3). Shell fragments (< 1.5 cm) are dominant and include cockle (30%) (Fig. 6a), mussel (10%) and oyster (10%). The majority of shell is unburnt and burnt fragments (~5%), where present (Fig. 6f), are mainly small (< 200 μm). Occasional unburnt fish bone is also present (Fig. 6b). Of particular interest are the bundles of needle-like calcite near the top of the profile (Fig. 6c and d), with single crystals also present in the groundmass. Dark charcoal and ash aggregates are common (no ash rhombs are visible), with the vertical arrangement on one side of the thin section (Fig. 6, TC_101) a result of smearing along the tube wall during sampling. Towards the base of the unit, slightly inclined and aligned charcoal and shell fragments may be indicative of trampling over a former ground surface (Fig. 6e).

4.3. Stratigraphic unit 2 (Samples TC102, TC103)

This unit is equivalent to the unit below the main shell-bearing midden unit as presented at the base of Box Core A and top of Box Core B. In the tube core it is approximately 15 cm thick, with a relatively sharp transition from the overlying shell midden and a more gradual transition to the underlying gyttja unit (Fig. 6). As indicated from the ASEM results (Fig. 6), quartz-rich sand rather than shell is the dominant phase in this unit, with cultural material still present in the form of bone (Fig. 6g) and charcoal. Acicular calcite is also present within the groundmass (Fig. 6h), possibly reflected by the high relative percentage of fine calcite (1.1%) in the ASEM analyses.

Table 3
Main stratigraphy and micromorphological characteristics of the (tube core) sediments adjacent to the midden excavation.

Unit/Facies	Description	Microstructure	Voids	c/f related distribution	c/f ratio	Coarse material				Fine fraction	Micromass b-fabric	Pedofeatures
						Shell	Rock	Bone	Charcoal			
1	Shell midden	Single grain - pellicular	simple - compound	coarse monic - gefuric	50:50	D	Vf	Vf	C	Grey	Striated (ash); Undifferentiated	Co (ash); pyrite framboids (Vf); needle-fibre calcite (Vf)
2	Sand (grey gyttja)	Pellicular	simple	chitonic	80:20	C	Vf - C	Fw	Fw	Grey to dark brown	Striated (ash); Undifferentiated	Co (ash); pyrite framboids (Fr)
3	Gyttja	Angular blocky	complex	coarse enaulic	40:60	Fw	Vf	Fw	C	Dark brown to black	Undifferentiated	HCo (Fe-, Mn-oxide); pyrite framboids (Fr)

Table abbreviations: Quantity. Vf: very few (< 5%); Fw: few (5–15%); C: common (15–30%); Fr: frequent (30–50%); D: Dominant (> 50%). Pedofeatures. Co: coatings; HCo: hypocoatings; No: nodules.

Excluding the large (1.5 × 2 cm) angular flint fragment (present in TC103), this unit has a low c/f ratio (Table 3) with an increasing silt component, and a more pellicular and compacted grain microstructure, with iron and manganese precipitates increasing towards the base of the unit. Interestingly the flint fragment contains a planktonic foraminifera (Karen Knudsen, pers. comm.) (Fig. 6i) and at least one calcareous alga (Marcus Key, pers. comm.) (Fig. 6j). Oyster and cockle shell fragments are present albeit in much lower proportions (~10%) than stratigraphic unit 1. Charcoal and plant pseudomorphs are also largely absent, except for a few fragments at the base of the unit (Fig. 6k).

4.4. *Stratigraphic unit 3 (Samples TC103, TC104)*

This gyttja unit was sampled to a depth of 20 cm, although based on previous coring (Skriver et al., 2017; Astrup et al. submitted) it likely goes to depths of 1 m or more. The unit generally shows an angular blocky structure, with partially accommodated and accommodated intrapedal cracks (Fig. 6, TC_104). However, this blocky/prismatic structure is most likely a result of drying in the oven rather than actual site structure, with the wet sediments otherwise showing a massive structure (see also Mijares, 2016). The minerogenic component comprises coarse sub-rounded to sub-angular sand and silt. Organics include meso-to macro-size plant tissue, with a moderate to weak laminar orientation, with some large fragments (up to 2 mm) showing visible internal structure (albeit insufficient to provide species identification). There is an increase in diffuse manganese and iron precipitates (e.g. Fig. 6m, 7n, 7) indicative of variable saturation of the sediments, and generally anoxic conditions. The latter is also reflected by abundant pyrite framboid aggregates in the groundmass (Table 3) and also high pyrite (0.55%) content from the ASEM analyses. There is no obvious horizontal orientation and packing of plant fragments that may indicate trampling, nor was any cultural material observed in this sample. However, cultural material has been described within gyttja deposits elsewhere on the site (Skriver et al., 2017; Astrup et al. submitted).

5. Microstratigraphy – Box core sample

5.1. *ASEM analyses*

When combined, the box core profiles through the main shell-bearing midden excavation show four/five main layers or sub-units, which are summarised in Table 4 and presented in Fig. 7. Larger clasts are predominantly shell (cockle, mussel and oyster), pebble-sized flint fragments (including some artefacts), charcoal (20–1000 μm) and bone (some burnt). The assemblage of minerals is relatively homogeneous throughout the sequence, comprising mainly quartz, carbonate, feldspar, amphibole and heavy minerals. Whilst the modal size of quartz (~340–430 μm) and orthoclase (~195–280 μm) remains fairly constant, modal abundance of each mineral phase changes through the profile (Table 2). Quantitative mineral analyses shows a similar modal abundance of minerals in the upper unit of the Box Core (BC101) as in the upper unit of the Tube Core (TC1-1), with 51–53% quartz, 29–34% calcite (shell), ~10% feldspar (orthoclase, anorthite, albite, plagioclase), 0.1–0.15% apatite (bone) (Fig. 7). Modal size of quartz and K-feldspar are also similar (Table 2). This implies these units correspond to the same stratigraphic unit or facies. The higher abundance of plant in the Box Core (7.5%) compared to the Tube Core (2.6%) corresponds with the known concentration of charcoal in the former.

Similarly, the grey sand unit in the Tube Core (TC1-3) shows a similar modal abundance to the lowermost sub-units of the Box Core profile (BC201 and BC202), with 75–80% quartz, 29–34% calcite, ~15% feldspar (orthoclase, anorthite, albite, plagioclase), 1–2% calcite, 4–8% plant, and 0.12–0.19% pyrite (Fig. 7) again reflecting a common stratigraphic unit or facies. The greatest difference is shown in the lower section of the shell layers (BC103), which shows much lower

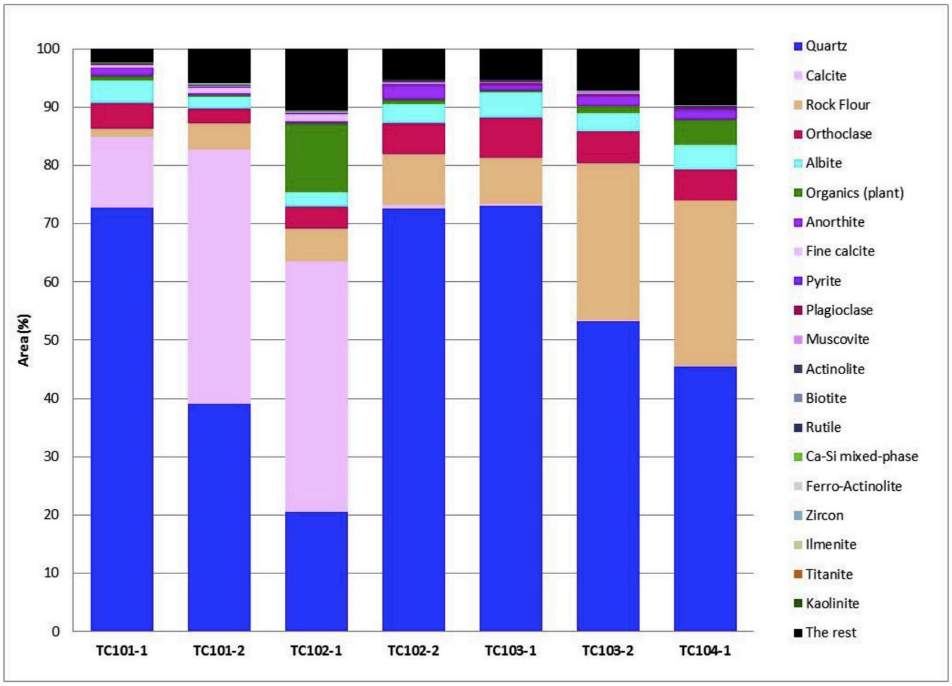

Fig. 5. ASEM modal mineralogy (calculated as pixel area) for identified sub-units in the tube core, with legend listing 21 of the total 28 mineral phases in order of relative abundance. The unidentified ('the rest') fraction comprises 7 mineral phases with an abundance below 0.01%.

abundances of quartz (32%) and higher abundances of calcite (47%), plant (12%) but with similar abundances of apatite (bone) (0.13–0.15%) as in other parts of the shell layers. The total porosity of the Box Core is much lower than the Tube Core (Table 2). However, this is attributed to compaction of a larger overall bulk following sampling compared to an auger sample and is not considered diagnostic. The defined microfacies (mF) and micromorphological description of the Box Core profile is provided below.

5.2. Sub-unit 1a (mF type 1a) (Sample BC101)

The charcoal sub-unit or microfacies type (mF type 1a, Figs. 4A, Figure 8) is characterised by a high c/f ratio, bridged grain microstructure with grains bridged in parts by grey-brown moderately laminated ash aggregates (no ash rhombs are visible) with embedded charcoal fragments, plant pseudomorphs, shell (Fig. 9a) and bone (Fig. 9b). Occasional fragments of detached and burnt fragments of the shell prism layer are present in some ash aggregates (Fig. 9b). Only a very few, small (~300 μm) sub-rounded cryptocrystalline rock fragments were observed. Charcoal fragments are mostly small (< 60 μm) but with a few larger (up to 2 cm) fragments, generally show some internal structure (e.g. Fig. 9c). Although plant species cannot be identified from a single cross-section, at least one represents elm (*Ulmus* sp.) (Fig. 9c) and others either alder (*Alnus* sp.) or hazel (*Corylus* sp.) (P.H. Mikkelsen, pers. comm. 2018). Both burnt and unburnt fragments of hard bone (< 5%) are present, including one or two (unburnt) spongy bone fragments (Fig. 9d). Despite the marine context, very few foraminifera were observed within the groundmass (Fig. 9e). A small brackish-water snail, possibly *Hydrobia* sp., was also identified (e.g. Fig. 9f).

5.3. Sub-unit 1b (mF type 1b) (Sample BC101, BC102)

This cockle/mussel sub-unit (mF type 1b, Fig. 8) contains a high frequency (40%) of whole cockle shell valves, with variable amounts of mussel (10%) (Fig. 9f) and oyster (10%) shell fragments. The latter two are more fragmented but the majority are interconnected (i.e. broken but *in situ*), with one or two mussel shells showing endolithic boring. In a few shells, the prism layer has been separated or detached (Fig. 9g), with a few smaller burnt fragments of this prism layer evident in the groundmass. Moderate to weakly striated ash aggregates, with embedded charcoal and plant pseudomorphs, burnt bone and/or fine minerogenic (mainly quartz) components, are often concentrated on the upper side of bivalve shells. Occasional fragments of burnt shell are also present within ash aggregates (Fig. 9h) but there is nothing to indicate high temperature combustion.

Also present are a few unburnt fragments of hard bone, including fish bone (Fig. 9i), spongy bone and unknown dark brown cellular fragments (Fig. 10). There is no reference for the latter but one possibility is that it is antler velvet. Although no deer velvet was observed at macroscale, bones of roe deer and tools made of antler are recorded in the midden (Astrup et al. submitted). The minor presence of impregnative iron-oxides associated with some ash features and as hypocoatings around minerogenic grains is possibly indicative of fluctuating redox conditions. Pyritic framboids are present as irregular aggregates around some shells and mineral grains but are not abundant.

5.4. Sub-unit 1c (mF type 1c and 1d) (Sample BC103)

This sub-unit is arguably made up of two main microfacies types, the first (mF type 1d) dominated by sub-horizontal oyster shell and well-sorted sands (Fig. 4B), and the second (mF type 1c, Fig. 8) comprising aggregates of charcoal, ash, shell fragments and moderately sorted sands (Table 4). As with the cockles, the oyster shells in mF type 1d are mainly complete or at least interconnected. Several show evidence of decalcification and separation of the calcitic prismatic layer, and many show evidence of endolithic boring (Fig. 9k). No foraminifera were observed but a micritic pelloid (Fig. 9l) is indicative of shallow-marine tidal conditions. Fabric pedofeatures include pyritic framboids, which occur as individual framboids and irregular aggregates within ash aggregates and on the edge of some shells.

Most plant fragments within the charcoal/ash microfacies (mF type 1c) show Class 2 or 3 weathering, although one charcoal fragment (Class 1) probably represents alder (*Alnus*) or hazel (*Corylus*) and

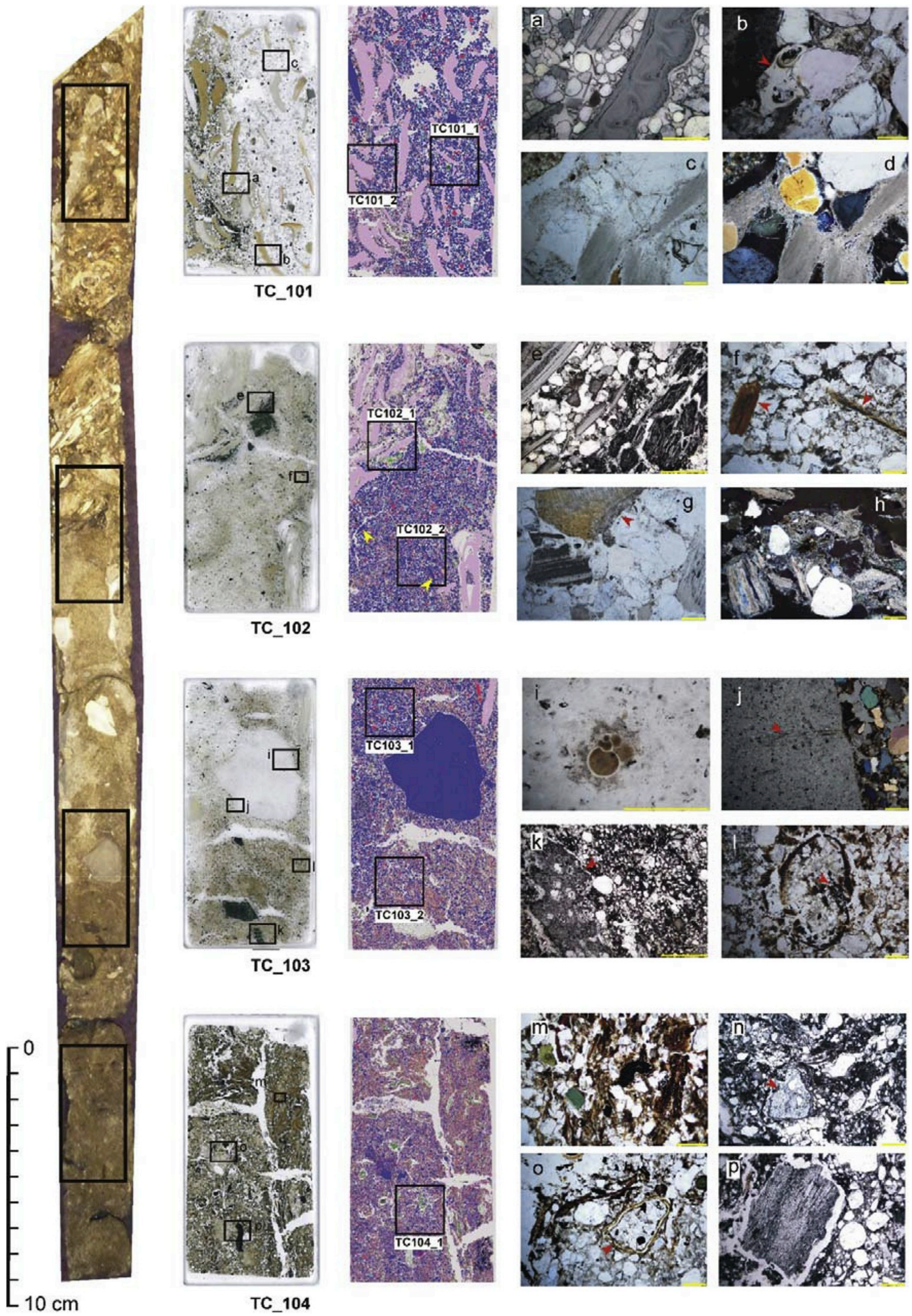

Fig. 6. Micromorphological sections and ASEM mineral maps of each from the tube core taken through the midden site (yellow scale bar is 300 µm in all slides). White arrows point to micro-fragments of flint. Thin section images show (a) cockle shell in sands with single grain microstructure (PPL, 600 µm), (b) unburnt fish bone (red arrow) within quartz sand, some possibly showing melting rims (?) (PPL, 200 µm), (c) acicular needle-fibre weathering of shell (PPL, 300 µm) (d) same as (c) (XPL, 300 µm), (e) accommodating charcoal fragments and bone fragments with fine ash coating on upper side (PPL, 600 µm), (f) burnt bone and fishbone(?) in sands with chitonic microstructure (PPL, 300 µm), (g), bone fragment (red arrow) in chitonic sand (PPL, 300 µm) (h) acicular calcite within groundmass (XPL, 300 µm), (i) planktonic foraminifera in flint fragment (PPL, 80 µm), (j) calcareous alga (red arrow) in flint fragment (XPL, 300 µm), (k) plant charcoal showing Class I degradation (PPL, 600 µm), (l), plant pseudomorph with pyritic framboids (red arrow) (PPL, 300 µm), (m) degraded plant material with green actinolite (PPL, 200 µm), (n) spongy bone fragment (red arrow) within plant fragments (PPL, 300 µm), (o) plant pseudomorph (red arrow) (PPL, 600 µm) (p) waterlogged plant fragment (PPL, 600 µm). (For interpretation of the references to colour in this figure legend, the reader is referred to the Web version of this article.)

another elm (*Ulnus*) or oak (*Quercus*) (P.H. Mikkelsen, pers. comm. 2018). Although much less abundant than the macro-scale record, a single hazelnut shell is observed in thin section (Fig. 9j). Ash aggregates are still evident along with burnt shell fragments (< 5%), burnt eggshell (1%), burnt bone (< 5%), as well as unburnt bone fragments (< 5%) and spongy bone (1%). A few small (< 300 µm) angular rock fragments (mainly quartz) were also observed.

5.5. Sub-unit 2a (mF type 2a) (Sample BC201)

Contrasting with the overlying shell units, this sub-unit or microfacies type (mF type 2a, Fig. 8) has a higher c/f ratio, an increasingly pellicular microstructure and poorly sorted minerogenic component (Table 4). Oyster shell fragments are infrequent (< 5%), but a cultural presence is still evident in the form of burnt bone (2%) (Fig. 9n), charcoal and plant pseudomorphs (< 5%), and cryptocrystalline flint fragments (~5%). One of these larger (1.5 cm) flint fragments shows heat damage in the form of fine cracks or 'crazing' (Fig. 9o), indicative of heating temperatures above 350 °C (Purdy and Brooks, 1971). Also present is an unknown organic, interpreted to possibly be antler velvet, (Fig. 9q). Towards the base of the unit, there are occasional fragments of seagrass, probably *Bangia* sp. (Fig. 9r), and increasing abundance of pyritic framboids.

Table 4
Main micromorphological characteristics and microfacies (mF) of the main midden sediments.

Sub-unit/mF type	Description	Microstructure	Voids	c/f related distribution	c/f ratio	Coarse material				Fine fraction	Micromass b-fabric	Pedofeatures
						Shell	Rock	Bone	Charcoal			
1a/mF 1	Charcoal	Bridged, grains bridged by ash	simple	gefuric	70:30	Fr	Vf	Vf	Fr	Grey	Parallel striated (ash); Undifferentiated	Co (ash); pyrite framboids (Vf)
1b/mF 1b	Cockle/mussel	Bridged, grains bridged by ash	simple	gefuric	60:40	D	Vf	Fw	C	Grey	Striated (ash); Undifferentiated	Co (ash); pyrite framboids (Fw)
1c/mF 1c	Charcoal/ash	Intergrain, bridged grains	complex	enaulic	40:60	Fw	D	Fw	C	Grey to black	Undifferentiated	Co (ash); impregnative Fe-, Mn-oxides; pyrite framboids (Fw)
1c/mF 1d	Oyster	Single grain	simple	coarse monic - chitonic	50:50	D	Vf	Fw	Fw	Grey	Undifferentiated	Impregnative Fe-, Mn-oxides; pyrite framboids (Fw)
2a/mF 2a	Sand	Increasingly pellicular	simple	chitonic	90:10	Fr	Fw	Vf	Fw	Grey	Granostriated in parts	HCo (Fe-, Mn-oxide) pyrite framboids (Fr)
2 b/mF 2b	Sand	Pellicular	simple	chitonic	80:20	Vf	Fw	Vf	Vf	Grey to brown	Undifferentiated	HCo (Fe-, Mn-oxide); No; pyrite framboids (C)

Table abbreviations: Quantity. Vf: very few (< 5%); Fw: few (5–15%); C: common (15–30%); Fr: frequent (30–50%); D: Dominant (> 50%). Pedofeatures. Co: coatings; HCo: hypocoatings; No: nodules.

5.6. Sub-unit 2b (mF type 2b) (Sample BC202)

The basal unit is a relatively massive sand unit and is distinguished from the overlying unit by an increased silt component and higher Fe- and Mn-oxide content. Presence of at least one pelloid (Fig. 9t) is indicative of shallow water conditions, with fragments of seagrass (Fig. 9s) indicative of the marine context. As in the overlying unit cultural presence is still evident from occasional knapped flint fragments (< 5%) - including one showing ‘crazed’ features (Fig. 9u), burnt bones (2%) (Figs. 4c and 9v) - including one fish bone (Fig. 9w), charcoal, and ash aggregates. A very discrete example of the latter at the base of the thin section shows a clear laminated structure (Fig. 9x). The single displaced and very degraded shell in this and in the overlying unit imply some or all of these cultural elements may derive from the overlying shell midden deposits.

6. Discussion

6.1. Cultural features of midden

The available chronology and macroscopic evidence of the Hjarnø Sund site provides a general sequence of subsistence collection, consumption, and disposal from about 7200 BP, followed by occupational abandonment after a 500 - 300 year period (Skriver et al., 2017; Astrup et al. submitted). This is comparatively short in relation to other large shell midden sites that record use up to 1000 years, perhaps reflecting greater constancy in their natural surroundings (Anderson, 2004). Macromorphological evidence indicates the Hjarnø midden site was located next to lagoonal deposits, with fragments of waterlogged wood within the gytta deposits indicative of drowned or displaced trees or branches from nearby woodland (Skriver et al., 2017). Although no cultural material was found in the gyttja of the tube core, previous excavations describe quite unique wooden and bone artefacts material within gyttja deposits elsewhere within the Hjarnø Sund site (Skriver et al., 2017; Astrup et al. submitted). These organic remains, along with bone, charcoal and ash, survive in the waterlogged, anoxic conditions indicated by the diffuse manganese and iron precipitates and sulphurous odour of the sediments. No ash rhombs are present and this likely reflects recrystallization of the ash in the wet alkaline sediments (Mallol et al., 2017). There is no visible compaction due to trampling in these organic deposits, although as Ismail-Meyer (2014) highlights, this may be due to swelling within the waterlogged conditions (and perhaps contrasts with terrestrial contexts). Compaction due to trampling can be seen more prevalently on the overlying shell deposits (see below).

At both the macro- and micro-scale there is evidence of flint artefacts, burnt and unburnt bones including fish bones, charcoal and ash that further attest to the midden's anthropogenic origins (see also Astrup et al. submitted). Macrofaunal evidence indicates both marine and terrestrial fauna are represented, with fish bones, particularly cod and flatfish, occurring in concentrations that suggest the use of specific areas of the midden for fish processing (Astrup et al. submitted; see also Anderson, 1989: 26). As in the Argus Bank site, fishing (and shellfishing) may have been a more important subsistence element than hunting (Fischer et al., 2007). Spongy (cancellous) bone tissue, possibly antler (Fig. 9d) and, by association, possible antler velvet (Fig. 10) are also present in both the cockle, mussel and oyster shell layers. There are no published examples of antler velvet, but any leather would be assumed to show some pore structure. Similarly any plant material would assume to show a more porous cellular structure. However, it is unknown what else these fragments could represent. Dense (cortical) bones survive better than spongy (cancellous) bones (Henderson, 1987), so the presence of spongy bone tissue at least, attests to the favourable preservation conditions of organic material in these submerged midden sediments.

Plant fragments cannot be identified definitively from a single cross-section but given that hazel (*Corylus* sp.) is the most frequent species

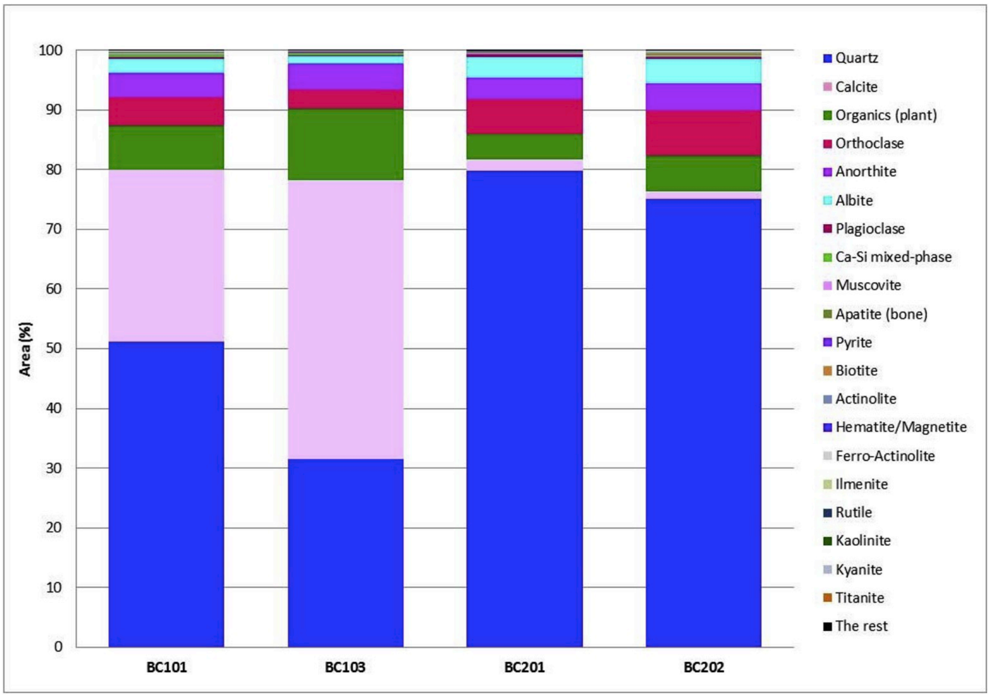

Fig. 7. ASEM modal mineralogy (calculated as pixel area) for identified sub-units in the box cores, with legend listing 20 of the total 27 mineral phases in order of relative abundance. The unidentified ('the rest') fraction comprises 7 mineral phases with an abundance below 0.04%.

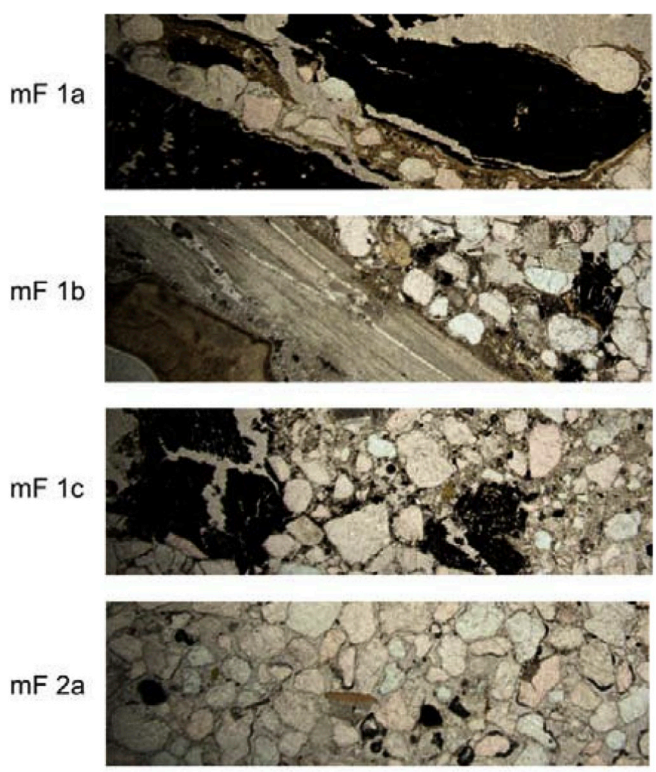

Fig. 8. Pictographs (PPL) of different microfacies (mF) types in the Box Core profile (refer also Fig. 4). Scale bar is 1 mm.

identified at the macro-scale, it is likely that the same species is represented by at least one of the charcoal fragments in thin section. Alder (*Alnus* sp.), hazel (*Corylus* sp.), elm (*Ulnus* sp.) and oak (*Quercus* sp.) are all contemporary species and were all used for firewood. Charcoal and plant fragments are variably preserved but because of their association with ash features, some of which preserve their laminated structure (e.g. BC101), are generally assumed to be associated with human activity and *in situ*. Given the low specific weight of charcoal (Macphail et al., 2010), it cannot be discounted that isolated fragments of charcoal may have been displaced. Indeed inverted chronologies from charcoal taken from the base (sample P4) and top (sample P1) of the 2016 excavations (see Astrup et al. submitted) imply some level of displacement of this material. Nevertheless, the charcoal and ash concentrated at the top of the box core profile (mF type 1a) must essentially be *in situ,* preserved through rapid burial. This may represent deliberately dumped material as the underlying sediments show no evidence of rubefaction from heating, although rubified substrates are not a ubiquitous feature of hearths in shell-matrix sites (Villagran, 2018) nor is it known whether rubified features would survive a long period of inundation.

Microfacies type 2 comprises both mussel *(Mytilus edulis* L.) and cockle, the former with an outer prismatic calcite layer, an inner aragonite (nacre) layer, and a definitive pink colour (Fig. 10b, see also Villagran et al., 2011a) whilst the latter are identified from their ridged surface and concave profile (Fig. 10c). They are distinguished from the oyster microfacies type because of their inclined or horizontal concave-up orientation and greater compaction (see also below), and in the latter correspond more to mF type A1 or mF type 4 of Villagran (2018). Regardless of shell type, very few have a preserved organic layer (pericostracum), possibly as a result of cooking at temperatures above 300 °C (Villagran et al., 2011b) and/or from degradation from organic acid in the soil (Villagran and Poch, 2014). However, disaggregated burnt fragments of the prismatic layers are observed (Fig. 8b). These may indicate burning of previously discarded shell and/or burning that occurred at higher temperatures, such as in a hearth laid over a bed of shell. Certainly the isolated ashes in association with the micro-sized charcoals, and high range of alterations of shell, and no visible alteration of substrate tend to support a 'fire-above' scenario and/or a dumped shell assemblage as described by Aldeias et al. (2016). Most likely it is a combination of these processes as unburnt interconnected prismatic layers (e.g. Fig. 8g) are also observed in the midden profile, and are indicative of carbonate dissolution.

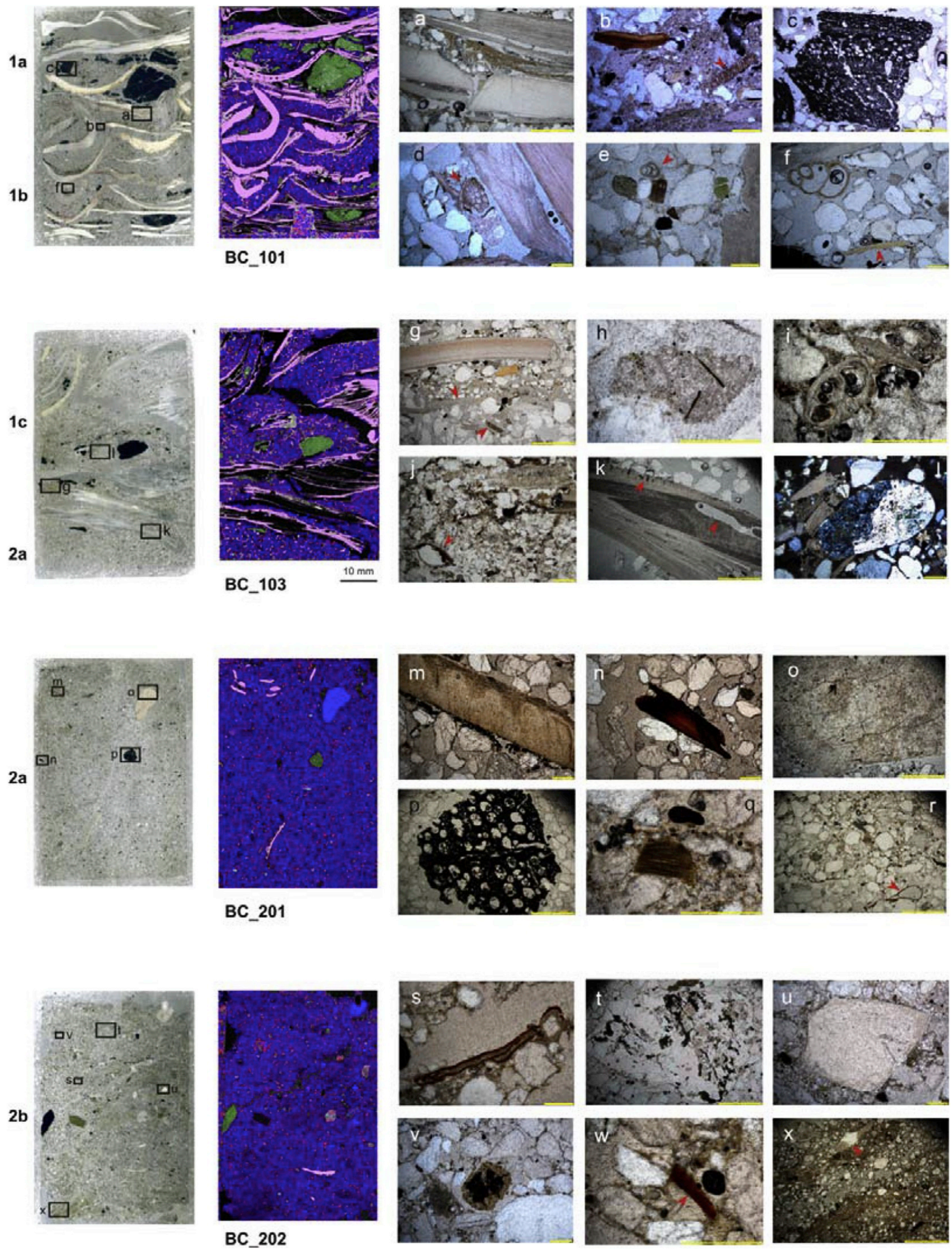

Fig. 9. Micromorphological sections from the Box Core A (yellow scale bar is 300 µm in all slides), showing (a) fragmented mussel shell and interstitial ash (PPL, 600 µm), (b) burnt and unburnt bone, burnt fragment of prismatic shell layer (red arrow) and plant fragments in ash overlying oyster shell (PPL, 200 µm), (c) charcoal fragment (PPL, 600 µm), (d) spongy bone (PPL, 300 µm), (e) foraminifera (red arrow) and possible antler velvet? in matrix of sub-rounded chitonic sands (PPL, 200 µm), (f) aquatic snail shell and burnt fish bone (red arrow) in monic sands (PPL, 300 µm), (g) separated prismatic layer of shell (red arrow, top) with burnt fragments of the prismatic shell layer (red arrow, below), (h) burnt eggshell in ash aggregate (PPL, 80 µm), (i) fish bone (PPL, 80 µm), (j) hazelnut shell (red arrow, PPL, 300 µm), (k) endolithic boring (arrow) in oyster shell (PPL, 600 µm), (l) pelloid (XPL, 300 µm); and Box Core B showing (m) ash accumulated below shell (PPL, 300 µm), (n) burnt bone fragment (PPL, 300 µm), (o) fine cracks ('crazing') within flint fragment (PPL, 600 µm), (p) charcoal (PPL, 600 µm), (q) possible antler velvet ? (PPL, 80 µm) (r) seagrass fragment (red arrow) with pyrite framboids developing in chitonic sands (PPL, 600 µm), (s) seagrass fragment (PPL, 200 µm), (t) pelloid (PPL, 600 µm), (u) angular flint fragment in quartz showing 'crazing' (PPL, 200 µm), (v) manganese alteration in bone (PPL, 300 µm), burnt fish bone (red arrow) (PPL, 80 µm), (x) laminated ash layers angular microfragment of flint (PPL, 600 µm). (For interpretation of the references to colour in this figure legend, the reader is referred to the Web version of this article.)

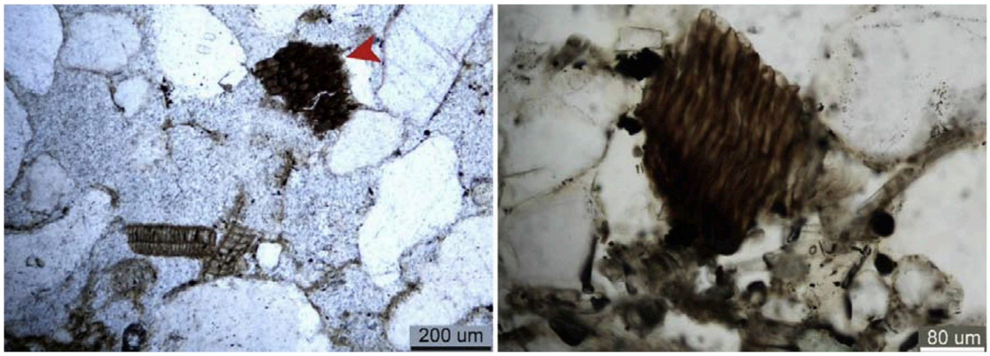

Fig. 10. Unknown organic fragments from BC102 (left) and BC103 (right) that is interpreted to possibly be antler velvet.

Fig. 11. Main shell types in midden, including A. cockle (*Cardium* sp., PPL, 600 μm), B. mussel (*Mylitis* sp., PPL, 300 μm), C. oyster (*Ostrea* sp., PPL, 600 μm). Note the dumbbell-shaped epizootic borings of in the oyster.

Observations (by PMA) of the macroscopic bone indicate the majority (> 90%) are unburnt and certainly most of the bones from the larger mammals show no traces of heating. The latter also applies at the microscopic level. What is notable is that many of the bones have been broken to get the marrow, and indeed the meat itself may have been cooked without affecting the bone. Bones that are evidently burnt bones are mainly fishbones, which have obtained a white - blue colour. Thin section shows hard bone fragments throughout the profile (e.g. Figs. 6f, 8b and n, w), many of which show reddish-brown colours and first-order interference colours that are indicative of heating to temperatures of 400 °C (Villagran et al., 2017). Thermal alteration of hydroxyapatite may have allowed better preservation of these burnt bone splinters (Villagran et al., 2011).

The oyster-rich layers correspond to the tossed shell microfacies (mF type F or mF type 3) of Villagran (2018), albeit with a slightly lower c/f ratio, and a dominance of subhorizontal shells and random orientation of bones and other small components. Oysters (*Ostrea edulis*) are almost wholly calcitic, with a thin outer prismatic layer, and most of the shell comprises a foliated structure (Fig. 11a). Whilst the low fragmentation and sub-horizontal distribution of oyster shells might indicate each of these microfacies represent a single tossing episode (Villagran, 2018), the interdigitation of these with charcoal/ash microfacies implies multiple episodes of shell discard within a period of several hundred years (Fig. 4). These charcoal/ash microfacies (mF type 1c, Fig. 8) show features that correspond to reworked hearth microfacies (mF type B) of Villagran (2018) with relatively abrupt contacts and absence of heated substrate.

Knapped lithic fragments also occur throughout the profile, even in the layers below the oysters, although the latter probably represent locally reworked material. These fragments are generally composed of cryptocrystalline chert (flint),[3] at least one of which had embedded fossils (Fig. 6i and j), although this is not unusual for this region. A few angular quartz fragments could also be cultural. Most lithic fragments show little or no alteration, however, at least three of these including one in sub-unit 2a (Fig. 9o) and two in sub-unit 2b show 'crazed' features from heating at high temperatures (> 350 °C) (Purdy and Brooks, 1971). Alongside the discrete burnt bone and charcoal in these grey sands below the shell midden, this could be interpreted as evidence for pre-midden occupation in the area before 7200 BP. Whilst smaller and more limited finds do occur beneath shell midden deposits (Anderson, 2004), in the absence of more comprehensive sampling it cannot be ruled out that these cultural features were displaced downwards through the profile as a result of mixing.

In summary, it can be argued that the shell deposits largely conform to the classification of Classen (1998, after Widmer, 1989) as a shell-bearing midden site, i.e. site composed of secondary refuse of many kinds of remains, including shell, generated by a wide range of activities, rather than simply a shell midden that shows no other activities. There is evidence of multiple shell building episodes, within each of which is additional evidence of discard of bone, including fish bone, and lithic material, some of which have been heated to high temperatures. Small pieces of worked flint (< 1 cm) found throughout the shell layers indicate activities took place directly on the shell-midden surface (Astrup et al. submitted). In addition there are accumulations of charcoal that may represent hearth features and/or discarded material from a hearth. Hence, as found in other midden sites (Anderson, 2004), multiple activities are being carried out on the surface of the shell heap. However, without further micromorphological analyses in other parts of the shell-bearing midden, it is not possible to define different functional areas as per Villagran et al. (2011a), nor to confirm the representativeness of the microstructure of the midden from the sampled profiles.

6.2. Formation history of shell midden

At the base of the midden sequence are the gyttja deposits that occur in extensive shallow and sheltered areas in many submerged Danish

[3] Calcareous alga are more prolific in Cretaceous flints than in Palaeozoic cherts but an exhaustive study of flint artefacts and geological samples revealed that such material is not particularly diagnostic and could have come anywhere from Denmark to southern Sweden (Kinnunen et al., 1985).

sites (Bailey et al. in press). Fine detrital gyttja occurs in deeper parts of the midden site area. Below and surrounding the shell midden, the gyttja is interdigitated and, in some parts, shows minor mixing with the glacial clay as evidenced from the ASEM results. In the sampled deposits, the detrital gyttja shows a gradational transition to the overlying anoxic grey sands, possibly in association with the increased sedimentation rates more regionally (Lewis et al., 2016). As outlined by Lewis et al. (2016) local sedimentation rates are likely to be heavily influenced by available source sediments, hydrodynamic processes and topographical features, such as the glacial clay bank around which the midden site is concentrated (Fig. 1).

Local variation within the midden site is also indicated by the difference in the stratigraphic sequence even in the parallel 2015 excavations, where inclined gyttja and grey sand units *overlie* the shell deposits (see Astrup et al. submitted; their Fig. 3b). ASEM analyses would provide a means to correlate across these sampled units, as evidenced for the shell and grey sands between the tube and box core samples. Unfortunately ASEM analyses are unable to differentiate between different types of carbonate,[4] hence shell species and hence different shell units are identified mainly from their external morphology and internal composition (Kobayashi, 1969). Nevertheless, ASEM is useful in helping to differentiate sub-units and microfacies – e.g. TC1-1 and BC101, TC1-3 and BC202, and generally providing a more accurate and empirical analysis of the sediment profile (see also Ward et al., 2018).

In the 2017 excavation profile, the transition between the sands and the overlying oyster (*Ostrea edulis)* shell layers is relatively sharp, indicating accumulation over a stable surface. Whilst there is clear evidence of decalcification of shells, the degree and concentration of 'sacrificial' shell or secondary carbonates at the base of the oyster layer is much less than occurs in many terrestrial shell middens (see Villagran, 2018). This preferential dissolution of basal carbonate reflects a gradient in physicochemical conditions through the midden profile, and its comparative absence in these submerged deposits implies they were unlikely to have been exposed for any great length of time for such gradients to develop. In its marine context, the midden and its cultural components are not only buffered by the presence of carbonate and siliceous clays but also by the seawater itself, even with ash present. Indeed the stability of cultural material and lack of authigenic minerals may partly result from the neutral to alkaline and slightly anoxic conditions, compared to more variable conditions in fully terrestrial contexts (e.g. Karkanas et al., 2000).

Marine borers in the inner part of the oyster shells indicate the midden was located close to the high water mark as such epizootic infestations cannot survive extended periods of aerial exposure (see also Ward and Maksimenko, 2019). The sub-horizontal and concave-down orientation of the oyster shells also support a hydrodynamic stable orientation, with a shallow water context indicated from the presence of pelloids at the base of the oyster layer and in the underlying grey (gyttja) sands. The low concentration of foraminifera indicates that infilling sands may have derived from local runoff or from subtidal sand banks and shoals. There is possibly some evidence for an earlier occupation in the localised laminated ash layers at the base of the box core profile (Fig. 9x), and presence of cultural material including burnt bone (Fig. 8w) and heated lithic fragments (Fig. 9u). More likely this cultural material derives from reworking within the saturated sandy sediments (sub-unit 2) in the early phases of accumulation of the oyster layer (sub-unit 1d), with a reworking distance of up to 10 cm indicated by the occasional displaced shell. There is currently no chronology from this pre-oyster phase, although a luminescence age estimate from the base of the 2017 excavation is forthcoming.

The continued accumulation of shell acted as a skeleton to minimise the amount of reworking. Rather reworking, or mixing of cultural and natural deposits, is largely confined to the siliciclastic layers above and to a much less extent below the shell-bearing midden layers. There is no evidence of major homogenisation of deposits and certainly no features that would be indicative of bioturbation in a terrestrial setting (e.g. excretion fabrics, chamber voids). In the micromorphological profile, discrete depositional phases of oyster and charcoal deposition (Fig. 4) imply continued use of the midden site (see also Claassen, 1991), with current age estimates from the oyster shells ranging between 7345 and 6860 cal BP (Astrup et al. submitted). These may or may not represent smaller spatial units of shell within the larger shell-bearing midden site (Anderson, 2004). Higher resolution chronology and additional micromorphological investigation, aided by ASEM analyses of adjacent deposits, is needed to confirm this observation.

The change in dominant species from oyster to cockle is well documented for this region but whether this reflects changing cultural traditions and/or regional trends in environmental change that affect mollusc habitats (e.g. sediments, salinity) is unknown (Lewis et al., 2016; Larsen et al., 2018; Astrup et al. submitted). Whilst the stratigraphy of the broader midden area shows an overall coarsening upwards sequence that is consistent with shallowing, the modal grain size through the oyster and cockle shell layers is fairly consistent around 450 μm (with a median grain size of 360 μm for quartz) implying a constant source and/or transport process. However, micromorphological evidence does provide evidence for a depositional hiatus or stasis between the accumulations of oyster- and cockle-shell. Minerogenic sands accumulating in and between the discarded oyster shells would have minimised the effects of trampling that otherwise would have resulted in greater fracturing of the oyster shells, but which is very evident in the mussel (*Mytilus edulis)* and cockle shells in the mid to upper layers of the midden profile (see also Ward and Maksimenko, 2019). The generally good preservation of the shell, minimal boring by epizootic fauna, and fewer iron and manganese precipitations in the sediments is indication that these layers accumulated in more oxic conditions.

Indeed parts of these shell layers may have accumulated above tide level, as implied by the needle-fibre weathering in the uppermost part of the tube core. According to Villagran and Poch (2014; see also Villagran, 2018), acicular calcite derives from physical weathering, specifically frost action, on the degrading shell matrix (specifically the surface nacre layer) of mussel (*Mytilus edulis* L.). The observation of similar needle-fibre calcite in the Hjarnø sediments, in a similar climatic context, is likely due to the same processes. During the warmer climatic conditions of the Holocene Thermal Maximum (8000–6000 BP; Rosentau et al., 2017), it is unlikely that the brackish-saline waters of Horsens Fjord would have frozen. The implication is that the deposits, at least in this part of the midden site, may have been exposed (i.e. above sea level) for some period of time before being submerged. Whether this acicular calcite also reflects abandonment (refer Villagran, 2018) is unknown.

Site abandonment may have occurred as a result of inundation, with some minor re-working of the topmost part of the midden before sands buried the midden and surface charcoal deposits and protected them from further erosion. In parts of the midden where shell had accumulated over gyttja, the weight of accumulated shell (and overlying sands) may over time have compacted these deposits and added to the submergence process. Overall indications are that the site originally formed at the lagoon foreshore and continued to accumulate there, even as the site began to become submerged. This does not discount the possible occupation of the supra-littoral zone at the same time, and indeed the combusted wood fragments must have originated from nearby woodlands.

The woodlands have now given way to farmland but below the water, the shell-bearing midden deposits have remained shallowly buried until the more recent erosion of these surface sands. The latter

[4] Preliminary unpublished ASEM analyses indicates small but detectable differences in the major element chemistry of eight reference shell samples that may be diagnostic of species and/or environment.

may be a result of loss of eel-grass (*Zostera marina*) (Rasmussen 1977) and/or changes in local currents (Skriver et al., 2017). It is also known that sand near the Hjarnø jetty was mined for building the foundations for the jetty extension, which itself may have limited longshore transport of sand and further exacerbated any regional effects of erosion. Regardless this recent erosion is impetus for ongoing research on the site, which is likely to continue to provide useful insights into the formation and inundation history of this and possibly other shell-bearing midden sites in Horsens Fjiord.

7. Conclusion

Along with other studies of Hjarnø Sund, this micromorphological study indicates there is high stratigraphic integrity of what is defined as a shell-bearing midden (shell-matrix) site, which all evidence indicates is anthropogenic in origin (with layers of natural deposition). Whilst the available chronology is fairly coarse, micromorphology provides evidence of more discrete layering within the midden profile as well as insights into both the cultural aspects of midden sites as well as its taphonomy. Although largely limited to a single profile, the micromorphological evidence indicates that the site represents conflations of discrete deposits at the water's edge, which remained stable and largely undisturbed by the process of inundation and complete submergence. Local minerogenic sands within and over the shell deposits have more than once helped stabilise the site up until more recent times. These stabilising sands are argued to be natural rather than cultural in origin, and in that regard may differ from some terrestrial shell-matrix sites (see Villagran, 2018).

This study also demonstrates the value of box core sampling in association with excavation of submerged archaeological sites. Much of the sedimentary matrix and especially fine material can be lost during excavation using suction methods. Hence micromorphology combined with ASEM not only helps address this but also provides a largely intact profile to explore sedimentary structures, fine mineralogical features, shell matrix elements and their cultural associations. Additional micromorphological analyses of other concentrated charcoal or hearth-like features within the Hjarnø site, aided by Fourier transform infared spectroscopy analyses of the shells and the sediments (see Aldeias et al., 2016), would help better assess the types of shellfish cooking methods used.

Similarly additional micromorphological investigation, aided by automated mineral analyses, of the stratigraphic units and microfacies across the site and over the wider area would aid cross-correlation of chronostratigraphic and archaeostratigraphic units and help assess whether the observations from this single study are more local or regional in nature. As previous studies have demonstrated, ASEM essentially provide a more accurate and empirical analysis of archaeological sediments, and a clear visual representation of mineral associations within these. Comparison with chronologically equivalent terrestrial shell-bearing midden sites and/or experimental work would also help clarify the conditions that preserve shell-matrix sites during inundation, and also the long and short-term the effects of marine inundation on cultural micromorphological features.

Acknowledgements

CRediT author statement: **Ingrid Ward**: Conceptualization, Methodology, Formal Analysis, Investigation, Original draft preparation, Review & Editing, Visualisation; **Peter-Moe-Astrup**: Supervision, Investigation, Resources, Writing – Review & Editing; **Kelly Merigot**: Formal Analysis, Software, Writing – Review & Editing. The authors wish to acknowledge the Australian Research Council, through the funding of the Deep History of Sea Country (Discovery Project DP170100812) to facilitate the international collaboration between Flinders University and Moesgaard Museum. The authors specifically wish to thank the DHSC team, and in particular Jonathan Benjamin and John McCarthy for their role in the design of the excavation, sampling and recording of the Hjarnø midden site. Moesgaard and Flinders provided resources and equipment. We also wish to thank Geoff Bailey and Jonathan Benjamin for edits on an earlier draft of the manuscript, and the anonymous reviewers for their helpful comments.

Appendix A. Supplementary data

Supplementary data to this article can be found online at https://doi.org/10.1016/j.jas.2018.12.009.

References

Aldeias, V., Bicho, N., 2016. Embedded Behavior: human Activities and the Construction of the Mesolithic Shellmound of Cabeço da Amoreira, Muge, Portugal. Geoarchaeology 31 (6), 530–549.
Aldeias, V., Gur-Arieh, S., Maria, R., Monteiro, P., Cura, P., 2016. Shell we cook it? An experimental approach to the microarchaeological record of shellfish roasting. Archaeological and Anthropological Sciences. https://doi.org/10.1007/s12520-016-0413-1.
Anderson, S.H., 1989. Norsminde: a "Køkkenmødding" with Late Mesolithic and Early Neolithic occupation. J. Dan. Archaeol. 8, 13–40.
Anderson, S.H., 2000. Kokkenmodinger (shell middens) in Denmark: a Survey. Proc. Prehist. Soc. 66, 361–384.
Anderson, S.H., 2004. Danish shell middens reviewed. In: Saville, A. (Ed.), Mesolithic Scotland and its Neighbours. Society of Antiquaries of Scotland, Edinburgh, pp. 393–411.
Anderson, S.H., 2013. Tybrind Vig: Submerged Mesolithic Settlements in Denmark, vol 77 Jutland Archaeological Society Publications, Højbjerg Jutland Archaeological Society.
Astrup, P. M., Skriver, C., Benjamin, J., Ward, I., Stankewicz, F., Ross, P., McCarthy, J., Baggaley, P., Ulm, S., Bailey, G., submitted. Underwater shell middens: excavation and remote sensing of a submerged Mesolithic site at Hjarnø, Denmark. J. Coast. I. Archaeol..
Bailey, G., Andersen, S. H., Maarleveld, T.J., (in press). Denmark: Mesolithic coastal Landscapes submerged. In: Bailey, G., Galanidou, N., Joens, H., Lueth, F. and Peeters, H. (Eds.) The Archaeology of Europe's Submerged Landscapes. Springer, Cham.
Benjamin, J., O'Leary, M., Ward, I., Hacker, J., Ulm, S., Veth, P., Bailey, G., 2018. Underwater archaeology and submerged landscapes in Western Australia. Antiq. Proj. Gallery 92 (363). https://doi.org/10.15184/ aqy.2018.103.
Claassen, C., 1991. Normative thinking and shell-bearing sites. Archaeol. Method Theor. 3, 249–298.
Claassen, C., 1998. Shells. Cambridge University Press, Cambridge, UK.
Fischer, A., Richards, M., Olsen, J., Robinson, D.E., Bennike, P., Kubiak-Martens, L., Heinemeier, J., 2007. The composition of Mesolithic food evidence from the submerged settlement on the Argus bank, Denmark. Acta Archaeol. 78 (2), 163–178.
Haberlah, D., Strong, C., Pirrie, D., Rollinson, G.K., Gottlieb, P., Botha, P.P.W.S.K., Butcher, A.R., 2011. Automated petrography applications in quaternary science. Quat. Australasia 28 (2), 3–12.
Henderson, J., 1987. Factors determining the state of preservation of human remains. In: Boddington, A. (Ed.), Death, Decay and Reconstruction: Approaches to Archaeology and Forensic Science. Manchester University Press, Manchester, United Kingdom, pp. 43–54.
Henderson, W.G., Andersen, L.C., McGimsey, C.R., 2002. Distinguishing natural and archaeological deposits: stratigraphy, taxonomy, and taphonomy of Holocene shell-rich accumulations from the Louisiana chenier plain. Palaios 17 (2), 192–205.
Hrstka, T., Gottlieb, P., Skála, R., Breiter, K., Motl, D., 2018. Automated mineralogy and petrology – applications of TESCAN integrated mineral analyzer (TIMA). J. Geosci. 63, 47–63.
Ismail-Meyer, K., 2014. The potential of micromorphology for interpreting sedimentation processes in wetland sites: a case study of a Late Bronze–early Iron Age lakeshore settlement at Lake Luokesa (Lithuania). Veg. Hist. Archaeobotany 23, 367–382.
Karkanas, P., Goldberg, P., Wiener, S., 2000. Diagenesis in prehistoric caves: the use of minerals that form in situ to assess the completeness of the archaeological record. J. Archaeol. Sci. 27, 915–929.
Kinnunen, K., Tynni, R., Hokkanen, K., Taavitsainen, J.-P., 1985. Flint raw materials of prehistoric Finland: rock types, surface textures and microfossils. Geol. Surv. Finl. Bull. 334.
Knappett, C., Pirrie, D., Power, M.R., Nikolakopoulou, I., Hilditch, J., Rollinson, G.K., 2011. Mineralogical analysis and provenancing of ancient ceramics using automated SEM-EDS analysis (QEMSCAN®): a pilot study on LB I pottery from Akrotiri, Thera. J. Archaeol. Sci. 38 (2), 219–232.
Kobayashi, I., 1969. Internal microstructure of the shell of bivalve molluscs. Am. Zool. 9 996-672.
Larsen, J.S., Philippsen, B., Skriver, C., Astrup, P.M., Borup, P., Mannino, M.A., 2018. From oysters to cockles at Hjarnø Sund: environmental and subsistence changes at a Danish Mesolithic Site. 60 (5), 1507–1519.
Lewis, H., 2007. Pile dwellings, changing lake conditions and sediment deposition: preliminary soil micromorphology study of cultural deposits from underwater sites at Lake Luokesas, Molėtai Region, Lithuania. J. Wetl. Archaeol. 7 (1), 33–50.
Lewis, J.P., Ryves, D.B., Rasmussen, P., Olsen, J., Knudsen, K.-L., Andersen, S.H., Weckström, K., Clarke, A.L., Andrén, E., Juggins, S., 2016. The shellfish enigma

across the Mesolithic-Neolithic transition in southern Scandinavia. Quat. Sci. Rev. 151, 315–320.

Macphail, R.I., Allen, M.J., Crowther, J., Cruise, G.M., Hiattker, J.E., 2010. Marine inundation: effects on archaeological features, materials, sediments and soils. Quat. Int. 214, 44–55.

Mallol, C., Mentzer, S.M., Miller, C.E., 2017. Combustion features. In: Nicosia, C., Stoops, G. (Eds.), Archaeological Soil and Sediment Micromorphology. John Wiley & Sons Ltd, pp. 299–330.

Mijares, A.S.B., 2016. Hukay, [S.l.]. The Nagsabaran shell midden site: a soil micromorphological approach 8 ISSN 0119–173X. Available at. http://ovcrd.upd.edu.ph/asp/article/view/4984, Accessed date: 1 November 2017.

Mörner, N.A., 1982. Gyttja. In: Beaches and Coastal Geology. Encyclopedia of Earth Science. Springer, Boston, MA.

Nicosia, C., Stoops, G., 2017. Archaeological Soil and Sediment Micromorphology. Wiley Blackwell.

Purdy, B.A., Brooks, H.K., 1971. Thermal Alteration of Silica Minerals: an Archeological Approach, vol 173. pp. 322–325.

Rosentau, A., Bennike, O., Uscinowicz, S., Miotk-Szpiganowicz, G., 2017. The baltic sea. In: Flemming, N.C., Harff, J., Moura, D., Burgess, A., Bailey, G.N. (Eds.), Submerged Landscapes of the European Continental Shelf: Quaternary Paleoenvironments. John Wiley & Sons, Chichester, pp. 103–133.

Salazar-Jimenez, A., Frey, R.W., Howard, J.D., 1982. Concavity orientations of bivalve shells in estuarine and nearshore shelf sediments, Georgia. J. Sediment. Petrol. 52 (2), 0565–0586.

Skriver, C., Borup, P., Astrup, P.M., 2017. Hjarnø sund: an eroding Mesolithic site and the tale of two paddles. In: Bailey, G.N., Harff, J., Sakellariou, D. (Eds.), Under the Sea: Archaeology and Palaeolandscapes of the Continental Shelf. Springer, Cham, pp. 131–143. https://doi.org/10.1007/978-3-319-53160-1_8.

Stoops, G., Marcelino, V., Mees, F., 2010. Interpretation of Micromorphological Features of Soils and Regoliths. Elsevier, Oxford.

Villagran, X.S., 2018. The shell midden conundrum: comparative micromorphology of shell-matrix sites from South America. J. Archaeol. Method Theor. https://doi.org/10.1007/s10816-018-9374-2.

Villagran, X.S., Balbo, A.L., Madella, M., Vila, A., Estevez, J., 2011a. Stratigraphic and spatial variability in shell middens: microfacies identification at the ethnohistoric site Tunel VII (Tierra del Fuego, Argentina). Archaeol. Anthropol. Sci. 3, 357–378.

Villagran, X.S., Balbo, A.L., Madella, M., Estevez, J., Vila, A., 2011b. Experimental micromorphology in Tierra del Fuego: building a reference collection for the study of shell middens in cold climates. J. Archaeol. Sci. 38, 588–604.

Villagran, X.S., Huisman, D.J., Mentzer, S.M., Miller, C.E., Jans, M.M., 2017. Bone and other skeletal tissues. In: Nicosia, C., Stoops, G. (Eds.), Archaeological Soil and Sediment Micromorphology. John Wiley & Sons Ltd, pp. 11–28.

Villagran, X.S., Poch, R.M., 2014. A new form of needle-fibre calcite produced by physical weathering of shells. Geoderma 213, 173–177.

Ward, I., Merigot, K., McInnes, B., 2018. Application of quantitative mineralogical analysis in archaeological micromorphology: a case study from Barrow Is., Western Australia. J. Archaeol. Method Theor 25 (1), 45–68.

Ward, I., Maksimenko, A., 2019. Marine micromorphology in 3D: Visualisation of a submerged midden site from Hjarnø, Denmark. J. Archaeol. Sci.: Report 23, 368–375.

Widmer, R., 1989. Archaeological Research Strategies in the Investigation of Shell Bearing Sites, a Florida Perspective. Annual Meeting of the Society for American Archaeology, Atlanta Paper presented at the.